Catalysis Today 171 (2011) 180–185

Contents lists available at ScienceDirect

Catalysis Today

journal homepage: www.elsevier.com/locate/cattod

Influence of sub-stoichiometric sorbitol addition modes on the structure and catalytic performance of alumina-supported cobalt Fischer–Tropsch catalysts

A. Jean-Marie[a,b], A. Griboval-Constant[a,**], A.Y. Khodakov[a,*], F. Diehl[b]

[a] Unité de Catalyse et de Chimie du Solide (UCCS), UMR 8181 CNRS, Université Lille 1-ENSCL-EC Lille, Bât C3, Cité scientifique, 59655 Villeneuve d'Ascq, France
[b] IFP Energies Nouvelles, BP3, 69360 Solaize Cedex, France

ARTICLE INFO

Article history:
Received 29 October 2010
Received in revised form 31 March 2011
Accepted 1 April 2011
Available online 7 May 2011

Keywords:
Clean fuels
Fischer–Tropsch synthesis
Cobalt catalyst
Promotion
Sorbitol

ABSTRACT

This paper focuses on the influence of different modes of sub-stoichiometric addition of sorbitol during catalyst preparation on the structure and performance of alumina-supported cobalt catalysts in Fischer–Tropsch synthesis. The catalysts are prepared using either alumina support pretreated with sorbitol or using co-impregnation of alumina support or using co-impregnation of calcined cobalt catalyst or catalyst post-treatment with sorbitol. It is found that the catalyst structure and catalytic performance are strongly affected by sorbitol addition mode. The catalysts prepared using support pretreatment with sorbitol or sorbitol addition during first impregnation step display an enhanced cobalt dispersion which is accompanied by a spectacular increase in Fischer–Tropsch reaction rate and hydrocarbon productivity.

1. Introduction

Fischer–Tropsch (FT) synthesis produces clean hydrocarbon fuels from natural gas, coal and biomass. Most of VIII group metals have measurable activity in carbon monoxide hydrogenation synthesis, but they yield different products: hydrocarbons, alcohols, acids, esters, etc. Cobalt supported catalysts have been particularly suitable for the production of long-chain hydrocarbons [1–4]. It is known that the catalytic conversion of carbon monoxide occurs on the cobalt metal sites. It has been shown that FT reaction rate is a function of cobalt dispersion, reducibility and catalyst stability. For cobalt particles larger than 6 nm, higher concentrations of cobalt metal sites typically favor higher FT reaction rates [5,6]. Deactivation is a major problem in FT synthesis and catalyst stability is also important to obtain higher hydrocarbon productivity [7,8].

Preparation of cobalt FT catalysts involves several essential steps. The catalysts for FT synthesis are commonly synthesized via aqueous impregnation of porous oxide supports (silica, alumina, titania, etc.) with the solutions of various cobalt salts [2,4,5], generally cobalt nitrate. The impregnation is followed by oxidative pretreatment at high temperature to decompose cobalt precursor. To obtain catalysts with higher cobalt contents, the catalysts are generally prepared in several impregnation steps (due to the restricted catalytic support porous volume and cobalt salt solubility). Cobalt oxide species are then reduced to cobalt metallic phase via thermal treatment with hydrogen. The catalyst structure is finally adjusted during FT reaction in an appropriate reactor where the catalyst is exposed to syngas. Due to a higher surface area, porosity and mechanical stability, alumina has been especially convenient for the design of cobalt FT catalysts even if its chemical stability under reaction condition is still a pitfall especially when unmodified alumina is used. Solid state reaction between alumina and cobalt oxides could also result in the mixed oxide phase (cobalt aluminate) which should be avoided since it does not catalyze FT synthesis. Minimization of concentration of hardly reducible cobalt aluminate and maximization of cobalt metal dispersion would enhance the catalytic performance.

Promotion with noble metals can solve many problems of alumina-supported cobalt catalysts such as reducibility; hydrocarbon selectivity, reaction rate and catalyst stability can also be affected [9]. Use of noble metals for catalyst promotion leads however to a significant increase in catalyst cost and can drive down the process efficiency.

It was shown recently [10,11] that the addition of different chelating molecules during catalyst impregnation could affect deposition of cobalt phases, cobalt dispersion, number of cobalt active sites in the reduced catalysts and catalytic performance. Girardon et al. [12] showed that introduction of small quantities of sucrose (saccharose) in the impregnating solutions enhanced cobalt dispersion and led to a higher catalytic activity of silica sup-

* Corresponding author. Tel.: +33 3 20 33 54 39; fax: +33 3 20 43 65 61.
** Corresponding author. Fax: +33 3 20 43 65 61.
E-mail addresses: anne.griboval@univ-lille1.fr (A. Griboval-Constant), andrei.khodakov@univ-lille1.fr (A.Y. Khodakov).

0920-5861/$ – see front matter © 2011 Elsevier B.V. All rights reserved.
doi:10.1016/j.cattod.2011.04.002

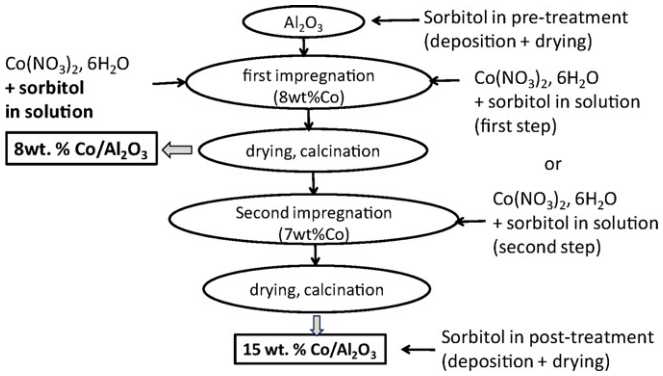

Fig. 1. Modes of sorbitol introduction in catalyst synthesis.

ported catalysts. Borg et al. [13] has recently uncovered that cobalt particle size and hydrocarbon selectivity of alumina-supported catalysts could be efficiently controlled by the addition of polyols (ethylene glycol and diethylene glycol). Other organic compound such as the ethylenediamine has been used by Dumond et al. [14] to prepare Co/Al_2O_3 catalysts. The mechanism of the modification of catalyst structure by using organic agents and their influence on the catalytic performance remain however rather erratic.

This paper explores the addition of sub-stoichiometric amounts of sorbitol for the preparation of alumina-supported cobalt catalysts. The catalysts were prepared using, either single or multiple step, impregnation(s) with and without sorbitol addition. Sorbitol was chosen because of its high solubility in water and because of its simpler structure in comparison with sucrose or glucose. The organic agent was added to cobalt catalysts at different key preparation steps. The catalysts have been characterized using a comprehensive set of characterization techniques. The catalytic performance in FT synthesis has been measured in a fixed bed microreactor at total pressure of 20 bar.

2. Experimental

2.1. Catalysts

The reference cobalt catalysts were synthesized via incipient wetness impregnation of alumina (Puralox SCCA 5/170, Sasol, pore volume = 0.47 $cm^3\ g^{-1}$, average pore diameter = 8 nm by BJH method) using aqueous solutions of cobalt nitrate. The cobalt content in the catalysts was respectively 8 wt.% (in single impregnation) and 15 wt.% (in two impregnation steps).

In some preparations the impregnating solutions contained also sorbitol (Aldrich). Sorbitol was added to the catalysts using 4 different modes: (i) directly to alumina support for support pretreatment; (ii) to the cobalt nitrate solution which was used to impregnate alumina support in the first impregnation step; (iii) to cobalt impregnating solution in the second impregnation step, (iv) to the calcined alumina-supported cobalt catalysts for catalyst post-treatment. The Co/sorbitol molar ratio was 6 for support pretreatment and 10 for co-impregnation; these ratios were chosen to avoid high exothermicity of sorbitol decomposition in air. Fig. 1 resumes the synthesis procedures. The catalysts obtained by co-impregnation are labeled as $x Co/Al_2O_3$-n-sorb where: x indicates the cobalt content (8 or 15 wt.%), n-sorb coimpregnation step (n = 1 or 2) involving sorbitol. The catalysts prepared using alumina pretreatement with sorbitol are designated as sorb-$x Co/Al_2O_3$, while the post-treated catalysts are labeled as $x Co/Al_2O_3$-post-sorb.

The impregnated catalysts were dried at 393 K and calcined at 673 K in a flow of dried air (heating ramp 1 K/min). For catalytic tests in fixed bed reactor the catalysts containing 8 wt.% of cobalt were impregnated to obtain the catalyst with 15 wt.% of cobalt using conventional procedure (without sorbitol), dried and calcined.

2.2. Catalyst characterization

The catalysts have been characterized by a wide range of techniques. Cobalt content was measured by X-ray fluorescence. The point of zero charge was measured by using a 0.1 M NaCl solution. 1.25 g of support was introduced to the volume corresponding to 23.75 g of NaCl solution. The volume was sealed and the suspension magnetically stirred for 24 h. After stirring, the pH of the solution was measured. Diffuse reflectance UV–vis spectra were obtained at ambient conditions with a Varian-Cary 4 spectrophotometer. DSC–TGA (10–15 mg sample loading) were carried out in a flow of air at heating rate of 1 K/min using DSC–TGA SDT 2960 thermal analyzer. X-ray powder diffraction experiments were conducted using a Bruker AXS D8 diffractometer using Cu(Kα) radiation for crystalline phase detection. The average crystallite size of Co_3O_4 was calculated using the 511 ($2\theta = 59.5^\circ$) diffraction lines according to the Scherrer equation [15]. Surface analyses were performed using a VG ESCALAB 220XL X-ray photoelectron spectrometer (XPS). The $Al_{k\alpha}$ non-monochromatized line (1486.6 eV) was used for excitation with a 300 W-applied power. The analyzer was operated in a constant pass energy mode (E_{pass} = 40 eV). Binding energies were referenced to the Al_{2p} core level (74.6 eV) of the Al_2O_3 support. Microstructural information was obtained from High Angle Annular Dark-Field Transmission Electron Microscopy (HAADF-TEM) using JEM-2100F JEOL microscope with resolution of 0.2 nm. An example of HAADF-TEM image for $8Co/Al_2O_3$-1-sorb catalyst is shown in Fig. 2. The average Co_3O_4 particle size was calculated from HAADF-TEM images using the volume-averaged particle size distribution histograms.

The reducibility of the catalysts was studied by temperature programmed reduction (TPR) using an AutoChem II 2920 apparatus (Micromeritics), 0.5 g of the sample was treated by a 5 vol.% H_2/Ar stream (3600 $cm^3\ h^{-1}\ g^{-1}$). The temperature was increased from room temperature to 1273 K at a rate of 2.5 K/min.

2.3. Catalytic measurements

Carbon monoxide hydrogenation was carried out in a fixed bed reactor operating at 20 bar, molar ratio $H_2/CO = 2$ and GHSV = 5 NL $h^{-1}\ g^{-1}$. The catalyst loading was 1 g. The samples

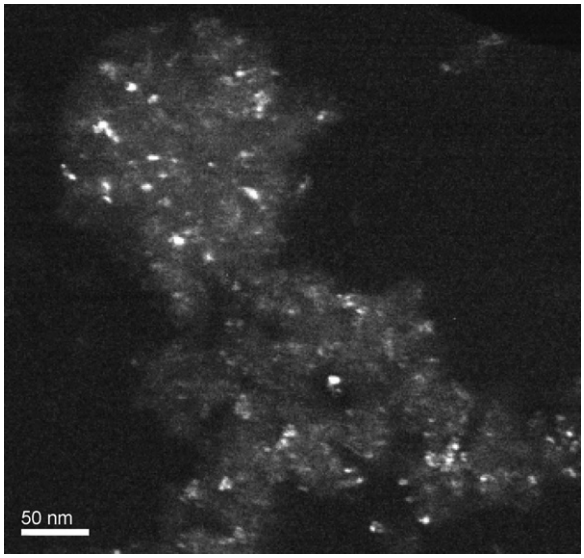

Fig. 2. HAADF-TEM image of $8Co/Al_2O_3$-1-sorb catalyst.

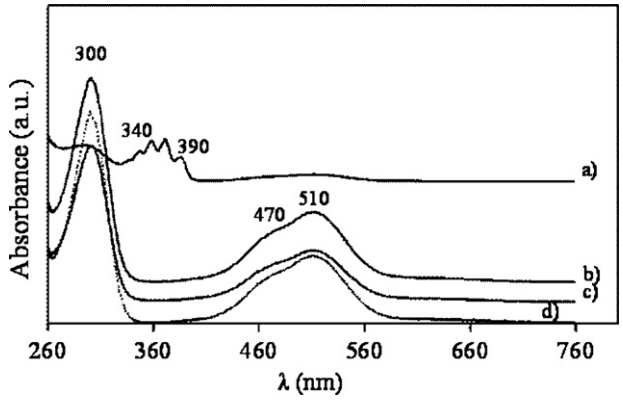

Fig. 3. UV–vis spectra of solutions ($C = 0.8\,mmol\,L^{-1}$): (a) cobalt nitrate + sorbitol + HNO_3 (Co/sor = 0.33), (b) cobalt nitrate + sorbitol (Co/sor = 0.33), (c) cobalt nitrate + sorbitol (Co/sor = 10), (d) cobalt nitrate.

were reduced in hydrogen flow during 10 h at 673 K with at GHSV = 2 NL h^{-1} g^{-1}. After the reduction, the catalyst was cooled down to 463 K and a flow of premixed synthesis gas was gradually introduced through the catalyst. Then, the temperature was slowly increased to 485 K. Gaseous reaction products were analyzed by on-line gas chromatography. Analysis of H_2, CO, CO_2 and CH_4 was performed using a packed CTR-1 column and a thermal conductivity detector. Hydrocarbons (C_1–C_7) were separated in a capillary Poraplot Q column and analyzed by a flame-ionization detector. High-molecular-weight products (C_7^+ hydrocarbons) and water were collected in two condensers thermostated at 423 K and 283 K respectively. The wax analysis was performed on a WCOT ULTIMETAL column (coating HT SIMDIST CB). The carbon monoxide contained 5% of nitrogen, which was used as an internal standard for calculating carbon monoxide conversion. Catalytic rates and selectivities were measured at steady state regime after 48 h time-on-stream. The reaction rates expressed in mol h^{-1} g^{-1}, were defined as the number of moles of CO converted per hour per gram of catalyst. Product selectivity (S) was reported as the percentage of CO converted into a given product expressed in C atoms. Carbon mass balances were respected within the margin of error of around 10% for all catalysts.

3. Results and discussion

3.1. Reference catalysts prepared without sorbitol

The reference $8Co/Al_2O_3$ and $15Co/Al_2O_3$ catalysts were prepared using single or two-step incipient wetness impregnation with solutions of cobalt nitrate. The UV–vis spectra of the impregnating cobalt nitrate solutions (Fig. 3) exhibit two broad bands at 470 nm ($^4T_{1g} \rightarrow {}^2A_{1g}$) and 510 nm (($^4T_{1g}$ (F) $\rightarrow {}^4T_{1g}$ (P)) typical of high-spin Co^{2+} ions in octahedral coordination [16–18]. Similar UV–vis spectra characteristic of isolated octahedral Co^{2+} ions were observed after cobalt deposition on alumina. In agreement with previous report [19] decomposition of cobalt nitrate in air was endothermic and proceeded between 408 and 458 K and led to formation of Co_3O_4 crystallites. The DSC–TGA curves of $8Co/Al_2O_3$ were similar to that observed in our previous report [20]. Cobalt particle size in the calcined catalysts was measured using XRD, XPS and TEM (Table 1). XRD and TEM suggest that cobalt oxide crystal size was 9.6 nm in the $8Co/Al_2O_3$ catalyst prepared using a single impregnation step, while in the $15Co/Al_2O_3$ catalyst prepared using two impregnation steps cobalt particle size was 12.4 nm. It is known that n_{Co}/n_{Al} atomic ratio determined by XPS also provides information about the sizes of cobalt oxide particles [2,21]. Higher concentration of cobalt detected by XPS suggests smaller sizes of cobalt oxide particles. Note that in agreement with XRD and TEM data, XPS n_{Co}/n_{Al} atomic ratio does not much increase with cobalt content: 0.06 compared with 0.05 respectively for $15Co/Al_2O_3$ and $8Co/Al_2O_3$ catalysts (Table 1). All these data indicate that cobalt introduced in the second impregnation of the reference $8Co/Al_2O_3$ sample does not probably contribute to the enhancement of metal dispersion. Moreover, it can be suggested that cobalt introduced in the second impregnation agglomerates preferentially on the Co_3O_4 particles already formed after the first impregnation step. This is also consistent with an increase in Co_3O_4 particle size observed by XRD and TEM after the second impregnation (Table 1): ~12 nm compared with ~9 nm for $15Co/Al_2O_3$ and $8Co/Al_2O_3$ catalysts respectively.

The TPR profiles of $15Co/Al_2O_3$ and $8Co/Al_2O_3$ catalysts (Fig. 4) exhibit three groups of hydrogen consumption peaks: low, medium and high temperature peaks. In agreement with previous reports [20,22–25] the low temperature peaks observed between room temperature and 650 K were mainly attributed to the reduction of Co_3O_4 to CoO. The small shoulder at 453 K seems to be related to the decomposition of residual un-decomposed nitrate species in hydrogen [20]. The second group of peaks situated between 650 and 1023 K is mainly attributed to the reduction of CoO particles to metallic cobalt and cobalt species interacting strongly with the support, while the high temperature peaks ($T > 1023$ K) could probably be attributed to the reduction of cobalt aluminate compounds and/or very small cobalt oxide particles. The fraction of barely reducible cobalt species (cobalt aluminate species or smaller cobalt oxide particles) in the catalysts was estimated from the relative area of high temperature TPR peaks (Table 1). Note that the shape of TPR profiles of $15Co/Al_2O_3$ and $8Co/Al_2O_3$ are almost identical. This suggests that increasing cobalt content from 8 to 15 wt.% in the reference catalysts does not change the relative fraction of easy reducible cobalt oxide phases (Co_3O_4) and hardly reducible cobalt species.

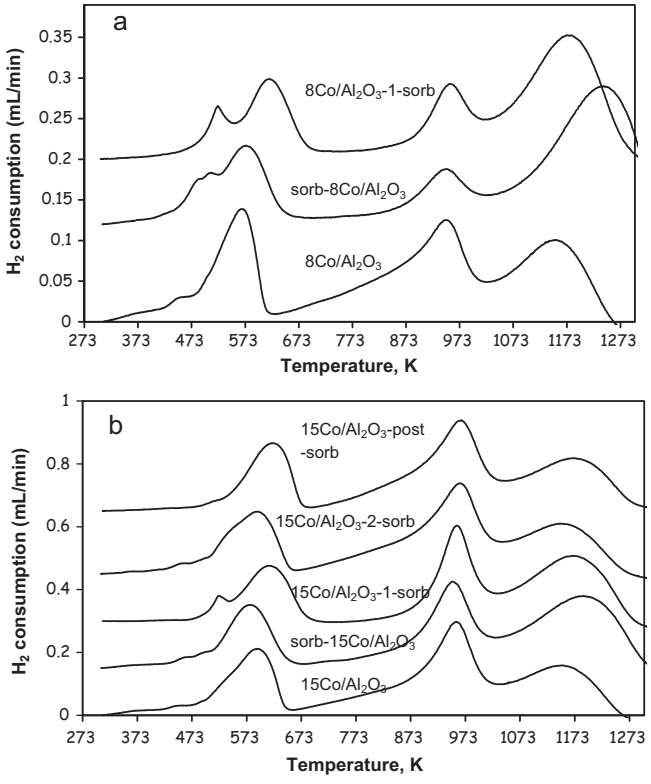

Fig. 4. H_2-TPR profiles of calcined catalysts with 8 wt.% (a) and 15 wt.% (b) cobalt content.

Table 1
Characterization of calcined cobalt supported catalysts.

Catalysts	Cobalt content, %	Sorbitol addition mode	Co/sor ratio	dCo_3O_4 XRD (nm)	XPS n_{Co}/n_{Al}	$d_{Co_3O_4}$ TEM (nm)	Fraction of barely reducible cobalt, TPR[a]
$8Co/Al_2O_3$	7.5	–	–	9.6	0.05	9.2	0.26
$15Co/Al_2O_3$	13.5	–	–	12.4	0.06	11.8	0.27
Sorb-$8Co/Al_2O_3$	7.9	Support pretreatment	6	<5	0.14	–	0.55
Sorb-$15Co/Al_2O_3$	13.8	Support pretreatment	6	7.5	0.15	–	0.41
$8Co/Al_2O_3$-1-sorb	7.6	First impregnation	10	<5	0.12	4.9	0.50
$15Co/Al_2O_3$-1-sorb	13.5	First impregnation	10	7.9	0.12	5.6	0.56
$15Co/Al_2O_3$-2-sorb	13.4	Second Impregnation	10	11.4	0.09	–	0.27
$15Co/Al_2O_3$-post-sorb	14.0	Catalyst post treatment	6	12.0	0.05	–	0.30

(nCo/nAl) monolayer = 0.15 for 8%Co and 0.3 for 15% Co.
[a] The fraction of barely reducible cobalt species is estimated from the relative intensity of high temperature TPR peak.

3.2. Catalysts prepared using alumina support pretreated with sorbitol

The alumina support was impregnated with sorbitol followed by drying at 493 K. Very small changes were observed in alumina after the impregnation. The point of zero charge of alumina was almost unaffected in the presence of sorbitol (PZC at pH = 8.3). Only very small modifications of BET surface area and porosity were also observed. The dried alumina pretreated with sorbitol was then impregnated with cobalt nitrate, dried and calcined in air to obtain sorb-$8Co/Al_2O_3$ catalyst. The support pretreatment with sorbitol results in dramatic enhancement of cobalt dispersion. Cobalt oxide particle size drops from 9 nm in $8Co/Al_2O_3$ to <5 nm in sorb-$8Co/Al_2O_3$ (Table 1). TPR (Fig. 4) data are consistent with these results. Thus, the smaller cobalt oxide particles have a much lower reducibility in sorb-$8Co/Al_2O_3$ than larger cobalt oxide particles in reference $8Co/Al_2O_3$ catalyst. The TPR data also show a significant increase in the intensity of high temperature hydrogen consumption peaks attributed to hardly reducible cobalt aluminate species (Table 1).

The second impregnation step conducted without sorbitol with sorb-$8Co/Al_2O_3$ catalyst to obtain sorb-$15Co/Al_2O_3$ does not result in significant modification of cobalt dispersion (Table 1). The cobalt oxide particle size slightly increases from <5 nm to 7.5 nm but remains very significantly smaller than in the reference $15Co/Al_2O_3$ catalyst (~12 nm). The TPR profiles of sorb-$15Co/Al_2O_3$ catalyst (Fig. 4) show some similarity with the reference $15Co/Al_2O_3$, while the concentration of barely reducible cobalt species is somewhat higher in the sorbitol-derived sample than in $15Co/Al_2O_3$. Thus, the second impregnation step conducted with the catalyst obtained from alumina pretreated with sorbitol allows keeping cobalt dispersion relatively high, while improves to some extent cobalt reducibility relative to sorb-$8Co/Al_2O_3$.

3.3. Catalysts obtained using co-impregnation of alumina support with sorbitol and cobalt nitrate

The alumina support was co-impregnated using the solution containing both cobalt nitrate and sorbitol. The UV–vis spectra of this solution are identical to those of cobalt nitrate (Fig. 3). They exhibit two broad bands at 470 nm and 510 nm typical for octahedral Co^{2+} ions and a band at 300 nm attributed to nitrate ions. This suggests that addition of this organic compound to the impregnating solution of cobalt nitrate does not considerably modify cobalt coordination. Sorbitol did not either have much influence of the pH; the cobalt nitrate solutions with and without sorbitol display pH at about 4.5. Note however that the UV–vis spectrum of cobalt nitrate in the presence of sorbitol shows significant changes when an oxidizing agent has been added. Fig. 3a presents the spectrum obtained in the presence of nitric acid with an organic compound/HNO_3 ratio of 3 and Co/sor = 0.33. Nitric acid is added first in the solution of sorbitol, and cobalt nitrate is added in a second step after 2 h at 313 K. Several bands appear in the range of 340–390 nm (Fig. 3a compared with Fig. 3c) corresponding to a transition ($^1A_{1g} \rightarrow {}^1T_{2g}$). This modification can be attributed to an oxidation of Co^{2+} into Co^{3+} ions due to the oxidation of sorbitol into organic acid by nitric acid and formation of metal complex [26–29].

Fig. 5 presents DSC–TGA curves in air flow during drying and calcination of the catalysts prepared from cobalt nitrate with sorbitol. Decomposition of cobalt precursor in the presence of sorbitol consists of two steps. It takes place differently compared to decomposition of cobalt nitrate without sorbitol [20]. The first decomposition step proceeds between 393 and 438 K. It is relevant to endothermic decomposition of cobalt nitrate. The second decomposition step is exothermic. It occurs between at 438 and 479 K. Sorbitol seems to have a major impact on the mechanism of cobalt precursor decomposition and decomposition temperature. It can be suggested that the exothermic decomposition step is related to decomposition of cobalt complexes with carboxylic acid produced by the oxidation of sorbitol (e.g. saccharic acid, gluconic acid) during drying and calcination. Indeed sorbitol oxidation to carboxylic acids was observed in relatively mild conditions in cobalt nitrate solutions.

Table 1 shows that cobalt particles in the dried and calcined catalyst $8Co/Al_2O_3$-1-sorb are much smaller than in the $8Co/Al_2O_3$ reference catalyst. This is consistent with previous results [12] obtained for silica supported cobalt catalysts prepared with the addition of sucrose. Addition of organic agent during impregna-

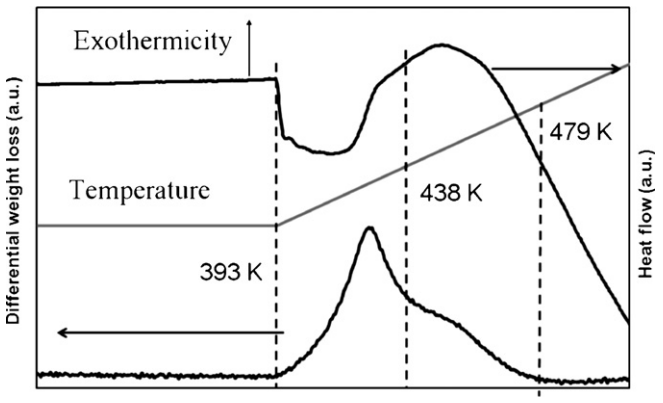

Fig. 5. DSC–TGA curves of $8Co/Al_2O_3$-1-sorb catalyst (temperature ramp = 1 K/min).

Table 2
Catalytic performance data (T = 485 K, 48 h on-stream, P = 20 bar, GHSV = 5 NL g^{-1} h^{-1}).

	Co/sor molar ratio	Sorbitol addition mode	X_{CO} %	FT rate (10^{-3} mol h^{-1} g^{-1})	S(CH_4) (wt.%)	S(C_{5+}) (wt.%)	α (C10–C70)
8Co/Al_2O_3	–	–	11.6	10.0	7	88	0.84
15Co/Al_2O_3	–	–	22.0	18.9	8	89	0.82
Sorb-15Co/Al_2O_3	6	Support pretreatment	61.1	52.5	8	87	–
15Co/Al_2O_3-1-sorb	10	First impregnation	45.6	39.2	7	89	0.88
15Co/Al_2O_3-2-sorb	10	Second impregnation	34.0	29.2	7	90	–
15Co/Al_2O_3-post-sorb	6	Post-treatment	29.8	25.6	6	90	0.88

tion results in the modification of cobalt precursor decomposition mechanism, higher exothermicity and higher cobalt dispersion. The observed enhancement of cobalt dispersion is consistent with TPR profiles (Fig. 4a) which are indicative of a lower reducibility of smaller cobalt oxide particles and of a higher concentration of hardly reducible cobalt species in the co-impregnated 8Co/Al_2O_3-1-sorb catalyst (Table 1).

The second step impregnation of the 8Co/Al_2O_3-1-sorb catalyst performed with cobalt nitrate and without sorbitol results in the 15Co/Al_2O_3-1-sorb catalyst with much higher cobalt dispersion than the reference 15Co/Al_2O_3 (Table 1). The cobalt oxide particle size in 15Co/Al_2O_3-1-sorb was almost twice smaller than in 15Co/Al_2O_3 catalyst. The TPR data (Fig. 4b) suggest similar fraction of easily reducible cobalt species after the introduction of cobalt nitrate in the second impregnation step. In fact, both cobalt dispersion and reducibility in 15Co/Al_2O_3-1-sorb is almost the same compared to their sorb-15Co/Al_2O_3 counterpart obtained using support pretreatment.

3.4. Catalyst prepared using co-impregnation of calcined cobalt catalysts with sorbitol and cobalt nitrate

The 15Co/Al_2O_3-2-sorb catalyst is obtained by co-impregnation of the 8Co/Al_2O_3 reference catalyst with the solutions containing cobalt nitrate and sorbitol followed by drying and calcination in air. We have seen previously that sorbitol introduction during the first impregnation step increases cobalt dispersion. In contrast, XRD and XPS results show a relatively small effect of sorbitol on cobalt dispersion when it is introduced in the second impregnation step (Table 1). Indeed, cobalt oxide particle size in 15Co/Al_2O_3-2-sorb is nearly the same as in the reference 15Co/Al_2O_3 (11.4 nm compared with 12.4 nm). Moreover, the TPR profiles of the 15Co/Al_2O_3-2-sorb catalyst (Fig. 4b) are almost exactly the same as for the reference 15Co/Al_2O_3 sample with similar fraction of hardly reducible cobalt species (Table 1). Thus, cobalt dispersion and reducibility seem not to be much affected by the addition of sorbitol to the impregnating solution during the second impregnation step.

3.5. Catalyst obtained using post-treatment with sorbitol

The post-treatment of cobalt catalysts was performed by adding sorbitol to the calcined 15Co/Al_2O_3 catalyst. Our goal was to uncover whether the catalyst post-treatment could modify to some extent cobalt dispersion. Indeed, very small influence of the post treatment with sorbitol on cobalt dispersion and reducibility was observed in post-treated 15Co/Al_2O_3-post-sorb (Table 1). Cobalt oxide particle size was the same in the reference 15Co/Al_2O_3 and in the 15Co/Al_2O_3-post-sorb catalyst. Almost identical TPR profiles were observed (Fig. 4b) showing similar concentration of hardly reducible cobalt species (Table 1). This suggests that the post treatment of alumina-supported cobalt catalysts with sorbitol does not have any noticeable influence on the cobalt dispersion and reducibility.

3.6. Catalytic performance of reference and sorbitol-derived catalysts

Table 2 displays catalytic performance data for 8Co/Al_2O_3 and 15Co/Al_2O_3 reference catalysts and for their counterparts prepared with sorbitol addition. The data were obtained after 48 h on-stream in a fixed bed reactor at total pressure of 20 bar, H_2/CO = 2, at 485 K and 5 NL h^{-1} g^{-1}. The reaction rate is expressed in mol of CO converted per hour and per gram of catalyst. FT reaction rates are almost proportional to cobalt content over the reference 8Co/Al_2O_3 and 15Co/Al_2O_3 catalysts. The 15Co/Al_2O_3 catalyst is almost twice more active than 8Co/Al_2O_3.

FT reaction rates over the catalysts prepared with the addition of sorbitol are strongly affected by the sorbitol introduction modes. Higher FT reaction rates were observed with the catalysts where sorbitol was added either for support pretreatment or in the first impregnation step. Higher FT reaction rate over these catalysts coincides with higher cobalt dispersion observed by characterization techniques. A much smaller effect was uncovered for the 15Co/Al_2O_3-2-sorb catalyst prepared using sorbitol addition during the second impregnation step or for 15Co/Al_2O_3-post-sorb catalyst post-treated with sorbitol. This also coincides with much lower effect of sorbitol on cobalt dispersion and reducibility in these catalysts. The results (Table 2) show similar methane and C5+ selectivity for all catalysts. In this work however, we do not discuss further the effect of sorbitol introduction modes on FT selectivity as catalysts were tested at different conversions.

The catalytic results are consistent with the characterization data. It is known that both cobalt dispersion and reducibility influence the number of active sites and catalytic performance of cobalt FT catalysts in fixed bed reactor. It is generally assumed that an increase in cobalt dispersion often coincides with a drop in cobalt reducibility. Indeed, smaller cobalt particles are usually more difficult to reduce than larger ones [2,23] and they could strongly interact with support. In this work higher hydrocarbon productivity is principally attributed to the enhancement in cobalt dispersion on sorbitol addition which occurs without significant detriment of reducibility. No increase in site-time yield could be expected however. Indeed according to the work by Bezemer et al. [6], the site-time yield should decrease rather than increase with higher cobalt dispersion. The best catalytic results in terms of cobalt time yield are obtained for catalysts prepared with sorbitol when the organic compound is introduced in pre-treatment or in the first impregnation step (Table 2). The influence of sorbitol added during the second impregnation step or catalyst post-treatment on catalyst structure and catalytic performance is less pronounced.

Cobalt dispersion in FT catalysts is strongly affected by cobalt phase nucleation and crystal growth phenomena. Our results show that sorbitol does not form complexes with cobalt ions in the impregnating solution. During oxidative pretreatments, e.g. drying or early phase of calcination, sorbitol can be oxidized to carboxylic acids such as saccharic or gluconic acids. DSC–TGA results suggest that the complexes formed by cobalt ions and organic acids have higher thermal stability than cobalt nitrate. Thus, these complexes could be possibly considered as additional cobalt oxide nucleation

sites for the crystallization of Co_3O_4 phase. Higher concentration of cobalt oxide nucleation sites in the sorbitol-derived catalysts would lead to smaller crystallites, higher cobalt dispersion and better catalytic performance.

4. Conclusion

Addition of sorbitol during the preparation of alumina-supported cobalt catalysts leads to significant modification of catalyst structure and catalytic performance in FT synthesis. The influence of sorbitol on cobalt dispersion, reducibility and FT reaction rate is strongly affected by sorbitol addition mode. Both alumina pretreatment with sorbitol or sorbitol addition during first impregnation step dramatically enhance cobalt dispersion while hinder to some extent cobalt reducibility. The catalysts prepared using alumina pretreatment with sorbitol or sorbitol addition during first impregnation step exhibited a spectacular increase in FT reaction rate. The influence of sorbitol added during the second impregnation step or catalyst post-treatment on catalyst structure and catalytic performance is less pronounced. These differences can be interpreted by different mechanisms of decomposition of cobalt precursor and crystallization of Co_3O_4 phase in alumina-supported cobalt catalysts.

Acknowledgments

The authors thank O. Gardoll, L. Byrilo, M. Tranteseaux-Frère, L. Sorbier, G. Cambien for assistance with characterization techniques. The authors are grateful to A.L. Taleb for TEM-HAADF measurements. The authors are indebted to IFP Energies Nouvelles for financial support of their work.

References

[1] Fischer–Tropsch technology, in: A. Steynberg, M. Dry (Eds.), in: Stud. Surf. Sci. Catal., vol. 152, 2004.
[2] A.Y. Khodakov, W. Chu, P. Fongarland, Chem. Rev. 107 (2007) 1692.
[3] B.H. Davis, Top. Catal. 32 (2005) 143.
[4] S.L. Soled, E. Iglesia, R.A. Fiato, J.E. Baumgartner, H. Vroman, S. Miseo, Top. Catal. 26 (2003) 101.
[5] E. Iglesia, S.C. Reyes, R.J. Madon, S.L. Soled, Adv. Catal. 39 (1993) 221.
[6] L.G. Bezemer, J.H. Bitter, H.P.C.E. Kuipers, H. Oosterbeek, J.E. Holewijn, X. Xu, F. Kapteijn, A.J. van Dillen, K.P. de Jong, J. Am. Chem. Soc. 128 (2006) 3956.
[7] A.M. Saib, D.J. Moodley, I.M. Ciobîcă, M.M. Hauman, B.H. Sigwebela, C.J. Weststrate, J.W. Niemantsverdriet, J. van de Loosdrecht, Catal. Today 154 (2010) 271.
[8] N.E. Tsakoumis, M. Rønning, Ø. Borg, E. Rytter, A. Holmen, Catal. Today 154 (2010) 162.
[9] F. Diehl, A.Y. Khodakov, Oil Gas Sci. Technol. 64 (2009) 11.
[10] T.P. Kobylinski, US Patent no. 4,088,671, Gulf Research & Development Co. (1978).
[11] C.C. Culross, C.H. Mauldin, US Patent no. 5,856,261, Exxon Research & Engineering Co. (1999); C.C. Culross, C.H. Mauldin, US Patent no. 6,136,868, Exxon Research & Engineering Co. (2000).
[12] J.-S. Girardon, E. Quinet, A. Griboval-Constant, P.A. Chernavskii, L. Gengembre, A.Y. Khodakov, J. Catal. 248 (2007) 143.
[13] Ø. Borg, P.D.C. Dietzel, A.I. Spjelkavik, E.Z. Tveten, J.C. Walmsley, S. Diplas, S. Eri, A. Holmen, E. Rytter, J. Catal. 259 (2008) 161.
[14] F. Dumond, E. Marceau, M. Che, J. Phys. Chem. C 111 (2007) 4780.
[15] B.D. Cullity, Elements of X-Ray Diffraction, Addison-Wesley, London, 1978.
[16] A.A. Verberkckmoes, B.M. Weckhuysen, R.A. Schoonheydt, Micropor. Mesopor. Mater. 22 (1998) 165.
[17] Y. Okamoto, K. Nagata, T. Adachi, T. Imanaka, K. Inamura, T. Takyu, J. Phys. Chem. 95 (1995) 310.
[18] M.G. Ferreira de Silva, Mater. Res. Bull. 34 (1999) 2061.
[19] J.-S. Girardon, A.S. Lermontov, L. Gengembre, P.A. Chernavskii, A. Griboval-Constant, A.Y. Khodakov, J. Catal. 230 (2005) 339.
[20] W. Chu, P.A. Chernavskii, L. Gengembre, G.A. Pankina, P. Fongarland, A.Y. Khodakov, J. Catal. 252 (2007) 215.
[21] F.P.J. Kerkhof, J.A. Moulijn, J. Phys. Chem. 83 (1979) 1612.
[22] D.G. Castner, P.R. Watson, I.Y. Chan, J. Phys. Chem. 94 (1990) 819.
[23] A.Y. Khodakov, J. Lynch, D. Bazin, B. Rebours, N. Zanier, B.B. Moisson, P. Chaumette, J. Catal. 168 (1997) 16.
[24] B. Ernst, A. Bensaddik, L. Hilaire, P. Chaumette, A. Kiennemann, Catal. Today 39 (1998) 329.
[25] A.Y. Khodakov, A. Griboval-Constant, R. Bechara, F. Villain, J. Phys. Chem. B 105 (2001) 9805.
[26] M.K. Eberhardt, C. Santos, M.Z. Soto, Biochim. Biophys. Acta 102 (1993) 1157.
[27] A.J. van Dillen, R.J.A.M. Terörde, D.J. Lensveld, J.W. Geus, K.P. de Jong, J. Catal. 216 (2003) 257.
[28] J.T. Cummins, T.E. King, V.H. Cheldelin, J. Biol. Chem. 224 (1957) 323.
[29] A. Blaskó, C.A. Bunton, E. Moroga, S. Bunel, C. Ibarra, Carbohydr. Res. 278 (1995) 315.